

Mixed bulk-filament nature in superconductivity of the charge-density-wave conductor ZrTe₃Kazuhiko Yamaya,¹ Shigeru Takayanagi,¹ and Satoshi Tanda^{1,2}¹*Center of Education and Research for Topological Science and Technology, Hokkaido University, Kita 13, Nishi 8 Kita-Ku, Sapporo 060-8628, Japan*²*Department of Applied Physics, Hokkaido University, Kita 13, Nishi 8 Kita-Ku, 060-8628 Sapporo, Japan*
(Received 26 July 2011; revised manuscript received 6 April 2012; published 11 May 2012)

We have shown that the superconducting transitions in ZrTe₃ are successive from filamentary to bulk, based on experimental results obtained for a superconducting specific-heat anomaly and the anisotropic superconducting transition curve of resistivity. A small jumplike superconducting specific-heat anomaly with a large and widely extended tail was observed to closely follow the anisotropic zero-resistance transition. We concluded that the jumplike anomaly signifies the onset of the long-range order of Cooper pairs with the opening of a superconducting gap at T_C , while the large and widely extended tail indicates behavior induced by Cooper pairs with a very short coherence length. As a limit for a very short coherence length, we propose local pairs with Bose characteristics. As a result, we can understand that the filamentary superconductivity is caused by the local pairs, and the large and widely extended tail is in a crossover region between superconductivity induced by local pairs and that induced by Cooper pairs. Based on a discussion about the origin of the change in the pair coupling from the starting of local pairing to Cooper pairing in ZrTe₃, we conclude that “mixed bulk-filament superconductivity” results from unique electronic structural changes in the quasi-1D + 3D (D, dimensional) Fermi surfaces after the CDW transition.

DOI: [10.1103/PhysRevB.85.184513](https://doi.org/10.1103/PhysRevB.85.184513)

PACS number(s): 74.25.Bt, 71.45.Lr, 74.25.F–, 74.70.Ad

I. INTRODUCTION

Superconductivity and charge density waves (CDWs) are cooperative electronic phenomena caused by Fermi surface (FS) instabilities and electron-phonon coupling. Superconducting transitions generally occur in three-dimensional (3D) electronic systems, while CDW transitions occur in low-dimensional electronic systems, but rarely in 3D systems. Indeed, CDW transitions have been observed in low-dimensional conductors such as layered MX₂ compounds and chain-based MX₃ compounds, where M is a group four or five metals and X = S, Se, or Te.^{1–5} A number of CDW compounds are also superconducting at temperatures lower than the CDW transition temperature (T_{CDW}) (this is called a CDW superconductor).^{1,5,6} The issue whether superconductivity and CDW states are competing or coexisting electronic states at low temperatures is a fundamental topic in condensed-matter physics.^{7–9}

Noteworthy among CDW superconductors is ZrTe₃, which exhibits a CDW transition around 63 K and superconductivity below 2 K. This is because ZrTe₃ has characteristic features regarding its FS topology^{10,11} and the nature of its superconductivity.^{5,12} Band-structure calculations for ZrTe₃ have predicted a 3D FS sheet, quasi-one-dimensional (1D) FS sheets, and a van Hove singularity (vHs) consisting of a quasi-1D FS intersecting a 3D FS (quasi-1D + 3D FSs). The topology of a quasi-1D + 3D FS is unique and is never seen in the FSs of chain-based compounds such as NbSe₃ and TaS₃.¹³ A quasi-1D FS sheet obtained by band-structure calculations forms a nesting vector consistent with the CDW vector obtained in electron microscopy and x-ray diffraction studies.^{14,15} A CDW gap driven by the nesting of the FS is observed on a quasi-1D FS in angle-resolved photoemission spectroscopy (ARPES) spectra, whereas no gap is observed on a 3D FS.^{16,17} Furthermore, the spectra at and near the vHs show no gap opening, but a large enhancement is

observed in the electronic density of states at the Fermi energy E_F , $D(E_F)$. The FSs that remain after the CDW formation, which are mainly 3D and quasi-1D + 3D FSs, are relevant to the superconductivity. Indeed, the superconducting transition of ZrTe₃ can be observed below 2 K by measuring the electrical resistivity and diamagnetic susceptibility.^{5,12} However, it has been concluded that the superconductivity is filamentary rather than bulk on the basis of results obtained for anisotropic superconducting transitions, which depend on the direction of applied currents and magnetic fields.¹² The filamentary behavior reported for NbSe₃¹⁸ is extrinsic, whereas the filamentary behavior observed for ZrTe₃ is intrinsic. However, the filamentary behavior observed for ZrTe₃ is uncommon if the FSs that remain after the CDW formation respond normally to superconductivity as found with as other CDW superconductors such as NbSe₂, Nb₃Se₄, and Cu_xTiSe₂, etc., because these all are bulk superconductors.^{19–21} Since resistivity and diamagnetic susceptibility measurements do not directly reflect the bulk properties of a sample, these properties must be detected directly to clarify the nature of the superconductivity in ZrTe₃.

In this paper, the temperature dependence of the specific heat of ZrTe₃ measured from 0.6 K up to 10 K is reported together with a reexamination of the anisotropic superconducting transition caused by electrical resistivity. A small jumplike superconducting specific-heat anomaly with an extended tail was observed to closely follow the anisotropic zero-resistance transition, showing successive superconducting transitions moving from filamentary at high temperatures to bulk at low temperatures below 2 K. We concluded that the jumplike anomaly signifies the onset of the long-range order of Cooper pairs with the opening of a superconducting gap at T_C , while the large and widely extended tail indicates superconducting behavior caused by Cooper pairs with a very short coherence length. As a limit for a very short coherence length, we

propose local pairs with Bose characteristics. And as a result, filamentary superconductivity is understood to be induced by local pairs, and the large and widely extended tail is understood to be a crossover region between local pairs and Cooper pairs. We show that “mixed bulk-filament superconductivity” is caused by a change in the pair coupling from local pairing with Bose characteristics to Cooper pairing. Based on a discussion of the origin of the change in pair coupling in ZrTe_3 , we conclude that the “mixed bulk-filament superconductivity” results from the unique electronic structural changes in the quasi-1D + 3D FSs after the CDW transition, where there is a large enhancement in $D(E_F)$ near the vHs and the simultaneous presence of narrow and wide bands at E_F .

II. EXPERIMENTS

Single crystals of ZrTe_3 were prepared by the iodine (I_2) vapor transport method. Starting materials were Zr sheets of 99.99% purity and Te ingot of 99.999%. The Zr sheets preheated in a vacuum and Te ingot were simultaneously reacted and transported with I_2 in a 2-cm-diam 20-cm-long quartz tube. After 14 days a number of single crystals up to $\sim 5 \times 8 \times 0.5 \text{ mm}^3$ were obtained at the cool end of tube. Two samples were used in the heat capacity measurements. Sample A consists of single crystals grown in the temperature gradient from 750 to 700 °C, and its total mass is 230 mg. While Sample B consists of single crystals grown in the temperature gradient from 730 to 680 °C, and its total mass is 200 mg. Each sample consists of 10 single crystals brought into thermal contact using Apiezon N grease (total mass of 20 mg).

The heat capacity from 0.6 to 10 K was measured with the heat pulse method using a conventional handmade ^3He cryostat. The sample temperature was determined using a calibrated resistance thermometer (Cernox Resistor, Lake Shore Cryotronics, Inc.). The overall accuracy was 2%, with a precision that was determined by performing measurements using two typical samples. One was a 200-mg standard aluminum (Al) plate of 99.99% purity (the superconducting transition temperature, $T_C = 1.21 \text{ K}$).²² The other was a 250-mg typical CDW superconductor NbSe_2 ($T_C = 7.22 \text{ K}$) that consisted of 13 single crystals contacted thermally as with the ZrTe_3 sample.²³ The total addenda (including the Cu-Be sample stage and the Apiezon N grease) amounted to nearly 20% of the total heat capacity.

For the resistivity measurement, the samples were selected from the single crystals of Samples A and B. Parallel-piped samples were cut from the same crystal. One was cut parallel to the a axis, and the other was cut parallel to the b axis. The resistance from 0.6 to 295 K was measured with the conventional dc-four-probe method. Carbon paste was used for the electrical contacts. The thermometer was a Cernox Resistor as in the heat capacity measurement.

III. RESULTS AND DISCUSSION

The room-temperature resistivities of ZrTe_3 were $\rho_a \simeq \rho_b = 3 \times 10^{-4} \Omega\text{cm}$, which are in good agreement with previously reported values.⁵ Figure 1 shows the temperature dependencies of the resistivities below 8 K for Samples A-1, A-2, B-1, and B-2. The resistivities were almost independent of

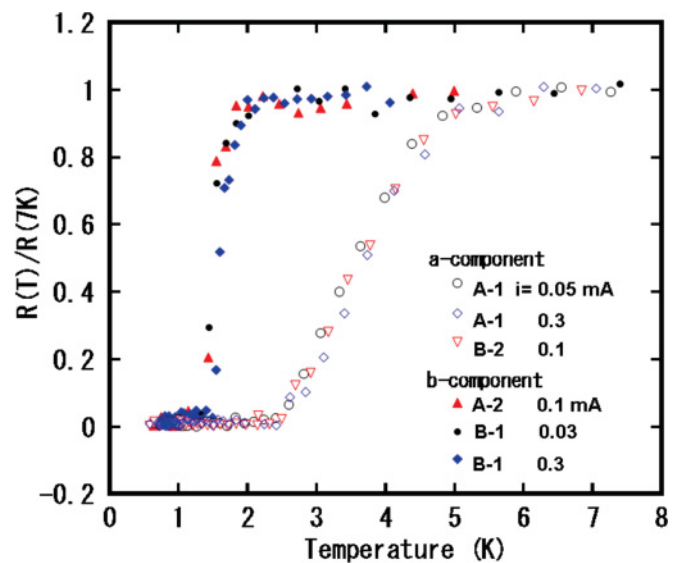


FIG. 1. (Color online) Temperature dependencies of the a and b components of resistivity of ZrTe_3 measured on samples A-1, A-2, B-1, and B-2.

current for the measured current values. The data agreed well within measurement accuracy, indicating good compositional homogeneity. An anisotropic superconducting transition was observed. The transition of the a component started at $\sim 5 \text{ K}$ and was broad ($\sim 2 \text{ K}$), while that of the b component was relatively narrow at only $\sim 0.6 \text{ K}$ from ~ 2.1 to $\sim 1.5 \text{ K}$. The b component did not exhibit any noticeable changes through the transition of the a component. The normal resistance of the b component showed a gradual decrease with decreasing temperature even when the a component exhibited zero resistance below 2.5 K. Both resistivity components became zero below 1.5 K. These results are almost the same as previously reported results,¹² suggesting the presence of filamentary superconducting channels along the a axis.

In addition to the anisotropic transition curves of resistivity, Nakajima *et al.* observed anisotropic ac diamagnetic susceptibilities depending on the direction of applied magnetic fields, which occurred at low temperature below the zero-resistance transition temperature.¹² They proposed a model in which the superconductivity of ZrTe_3 is filamentary, but not bulk. According to the model, superconducting filaments are aligned parallel to the a axis with the spacing of about 40 Å, and they are coupled weakly each other. However, with decreasing temperature the coupling becomes stronger. A zero-resistance transition along the perpendicular direction is observed at lower temperature. However, the origin of filamentary superconductivity remains unclear.

In contrast to the resistive transition result, specific-heat measurements $C_p(T)$ show unambiguous evidence of bulk superconductivity. Figure 2 shows the specific heat divided by temperature, C_p/T as a function of T^2 for Sample B. C_p/T decreases linearly with decreasing T^2 ; that is, it is well represented as a function of $C_p/T = \gamma + \beta T^2$ observed in $C_p(T)$ of a typical normal metal. Here γ is an electronic specific-heat coefficient, and β is a lattice specific-heat coefficient. Figure 2(b) shows that at around 2 K C_p/T deviates from the linear relation for T^2 observed in the high-temperature

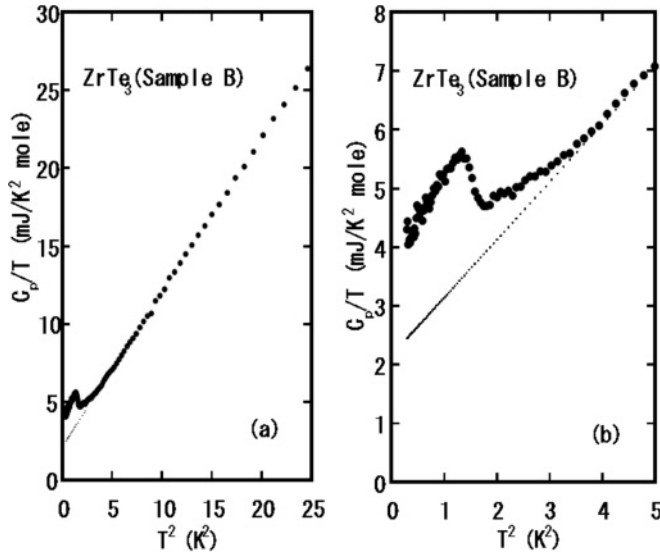


FIG. 2. (a) Temperature dependence of specific heat $C_p(T)$ of ZrTe_3 (sample B) plotted as C_p/T vs T^2 . The dotted line is a least square fit (see text). (b) C_p/T vs T^2 for $T^2 < 5 \text{ K}^2$ ($T < \sim 2.2 \text{ K}$).

range, then rapidly increases near 1.4 K, and beyond a peak at 1.2 K it gradually decreases. The humplike anomaly of C_p/T emerges below the zero-resistance transition temperature. The same result was obtained with Sample A. Here it should be noted that the temperature at which the specific-heat anomaly emerges corresponds well with that of the previously reported ac diamagnetic susceptibilities.^{5,12} This strongly indicates that the superconductivity of ZrTe_3 is thermally and magnetically bulk at low temperatures below 2 K.

When we compare the temperature dependences of both the specific heat and the resistivities, three main features can be summarized as follows. The first is that no specific-heat anomaly is observed in the zero-resistance transition region of the a component (between ~ 2.5 and $\sim 5 \text{ K}$). The second is that the deviation from the linear T^2 dependence of C_p/T is near the onset of the zero-resistance transition of the b component. The third is that the specific-heat anomaly rapidly increases around a temperature corresponding to the zero resistance of the b component (T_{0b}), and the peak of the specific-heat anomaly is below T_{0b} . The comparison shows that superconducting filaments aligned parallel to the a axis are coupled weakly to each other in the high-temperature region,¹² but with decreasing temperature the coupling becomes stronger with an increasing volume of superconducting filaments. Bulk superconductivity is induced over the entire sample at low temperature. Thus, we find successive superconducting transitions ranging from filamentary behavior at high temperatures to bulk behavior at low temperatures below 2 K. This contrasts with the case of TaSe_3 , which is known to be a filamentary superconductor that exhibits no bulk characteristics even at low temperatures below 1 K,^{24,25} except in recently published work on ring-shaped crystals of TaSe_3 .²⁶ Hence, we conclude that ZrTe_3 exhibits mixed bulk and filamentary superconductivity, but is neither bulk nor filamentary. This is a new type of superconductivity, which can be called “mixed bulk-filament superconductivity.”

Let us now discuss the values of γ and β of a function of $C_p/T = \gamma + \beta T^2$ determined by the least-square method. The dotted line in Fig. 2 represents calculated values of C_p/T with $\gamma = 2.15 \text{ mJ/mol K}^2$ and $\beta = 0.985 \text{ mJ/mol K}^4$ determined in the 3 to 6 K temperature range ($T^2 = 9 \sim 36 \text{ K}^2$) for Sample B. For Sample A, the obtained values were $\gamma = 2.23 \text{ mJ/mol K}^2$ and $\beta = 0.97 \text{ mJ/mol K}^4$, showing good agreement between the two samples. It should be noted that with ZrTe_3 , the γ value is obtained in the metallic CDW state below $T_{\text{CDW}} (= 63 \text{ K})$, but not in the normal metal state above T_{CDW} . The γ value obtained here is expected to be proportional to $D(E_F)$ on the remaining FSs after CDW formation, $D(E_F)_{\text{CDW}}$, but not $D(E_F)_{\text{metal}}$, which is $D(E_F)$ in the normal metal state. In fact, the decrease in $D(E_F)$ due to the CDW transition has been estimated by Chung *et al.*²⁷ We try to estimate the relative change in $D(E_F)$ caused by the CDW transition, $D(E_F)_{\text{CDW}}/D(E_F)_{\text{metal}}$ from the size of the resistance anomaly at T_{CDW} using an α parameter introduced by Kawabata; $D(E_F)_{\text{CDW}} = (1 - \alpha)D(E_F)_{\text{metal}}$.⁹ The α value of ZrTe_3 obtained here is $\simeq 0.4$, which is in good agreement with the reported values.⁸ Hence, $D(E_F)_{\text{CDW}}/D(E_F)_{\text{metal}}$ is $\simeq 0.6$. This is nearly three times as large as that of NbSe_3 , which is a CDW conductor, but not a superconductor.⁹ The large value of $D(E_F)_{\text{CDW}}/D(E_F)_{\text{metal}}$ may be due to the existence of the vHs, which may make superconductivity possible at low temperature.

To investigate the electronic states of bulk superconductivity of ZrTe_3 , we estimate the electronic specific heat $C_e(T)$ by subtracting the phonon contribution (βT^3) from $C_p(T)$ in the normal state, that is, $C_e(T) = C_p(T) - \beta T^3$, assuming no change in the phonon contribution in the superconducting state. Figure 3 shows C_e divided by temperature and γ , $C_e/\gamma T$ as a function of the normalized temperature, t_N , here $t_N = (T - T_C)/T_C$, and T_C is the temperature corresponding to the peak of $C_e(T)$ ($T_C = 1.17 \text{ K}$ for Samples A and B). Data of Al ($T_C = 1.15 \text{ K}$) that is a typical BCS bulk superconductor are added for comparison. The γ values used

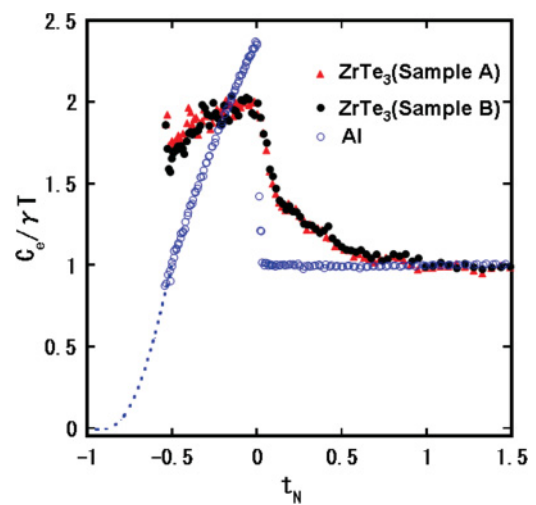


FIG. 3. (Color online) Temperature dependencies of electronic specific heat $C_e(T)$ of ZrTe_3 (samples A and B) plotted as $C_e/\gamma T$ vs t_N , where t_N is the normalized temperature by T_C [$t_N = (T - T_C)/T_C$] and γ is an electronic specific-heat coefficient in the normal state (see text). Al data are added for comparison. The dotted line represents a curve calculated using the BCS theory.

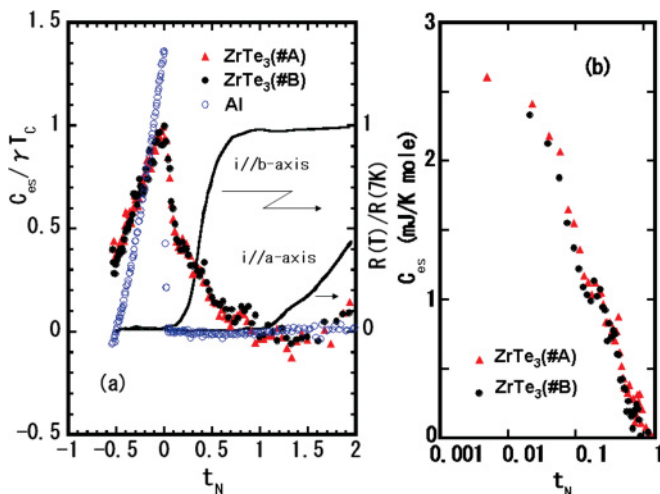


FIG. 4. (Color online) (a) Temperature dependencies of superconducting electronic specific-heat $C_{es}(T)$ of ZrTe₃ (samples A and B) plotted as $C_{es}/\gamma T_C$ vs t_N . Al data are added for comparison (see text). The temperature dependencies of resistivity normalized by 7 K (solid lines) refer to the right axis (see Fig. 1). (b) Temperature dependencies of $C_{es}(T)$ of ZrTe₃ (samples A and B) are plotted on a semilogarithmic scale.

are obtained in the metal state for Al ($\gamma = 1.24$ mJ/mol K²) and in the CDW metal state for ZrTe₃. We can see large differences when we compare the results of ZrTe₃ and Al. Al exhibits typical behavior of a BCS superconductor; that is, $C_e(T)$ shows a jump at T_C and falls below the γ value at low temperatures of $t_N < -0.5$ ($T < T_C/2$). The jump of the specific heat $\Delta C_e(T_C)$ was ~ 1.74 mJ/mole K, and the parameter $\Delta C_e/(\gamma T_C)$ was calculated as ~ 1.36 , which is close to the BCS value of 1.43. On the other hand, $C_e/\gamma T$ of ZrTe₃ exhibits a humplike anomaly with an extended tail above T_C . To estimate the unclear jump at T_C of ZrTe₃, we used the difference between C_e at T_C and γT_C [$\Delta C_e = C_e(T_C) - \gamma T_C$]. The $\Delta C_e(T_C)$ values of Samples A and B were ~ 2.30 and ~ 2.13 mJ/mole K, respectively. The parameter $\Delta C_e/(\gamma T_C)$ obtained of Samples A and B were 1.03 and 0.99, respectively, which were $\sim 30\%$ smaller than the BCS value. $C_e/\gamma T$ below T_C gradually decreases with decreasing temperature, and its value remains about 1.6 times higher than the γ value even at low temperatures of $t_N < -0.5$ ($T < T_C/2$). An extrapolation to $T = 0$ K of $C_e/\gamma T$ seems to be nonzero (a residual electronic specific heat, $\gamma_0 \neq 0$), although the measurement of $C_e/\gamma T$ in ZrTe₃ is needed down to well below $T_C/2$. This is in contrast to the exponential temperature dependence of $C_e/\gamma T$ in Al calculated by the BCS theory as shown by the dotted line in Fig. 3. Unconventional behavior such as the reduced value of $\Delta C_e/(\gamma T_C)$, the $\gamma_0 \neq 0$ and the extended tail suggest that ZrTe₃ is a non-s-wave superconductor.^{28–31}

The most interesting feature as regards the specific-heat anomaly is the extended tail above T_C . To determine the T dependence of the extended tail, the specific-heat anomaly caused by the superconducting transition $C_{es}(T)$ may be obtained from an extrapolation of the temperature dependence of $C_e(T)$ in the normal state. This extrapolation allows $C_{es}(T)$ as the difference between $C_e(T)$ and γT , $C_{es}(T) = C_e(T) - \gamma T$. Figure 4(a) shows the T dependencies of C_{es} normalized by

γT_C as a function of t_N . The resistivities normalized by 7 K are shown by solid lines for comparison. A jumplike anomaly is observed in the vicinity of T_C , and an extended tail is observed above $t_N \sim 0.1$. Figure 4(b) shows the T dependencies of C_{es} by a semilogarithmic plot. The temperature dependence of the extended tail is almost logarithmic, indicating superconducting fluctuations. C_{es} deviates from the $\log T$ dependence around $t_N \sim 0.1$, and then rapidly jumps very near T_C , signifying the onset of a long-range order of Cooper pairs with the opening of a superconducting gap at T_C , although the magnitude of the jump of C_{es} is fairly small compared with that of a BCS superconductor. Here, it should be noted that the superconducting fluctuation region appears from a temperature near $t_N \sim 1.0$, and the magnitude of the extended tail reaches nearly 50% of the peak value of C_{es} ; it is a large and widely extended tail. Such large fluctuations have never previously been observed in s-wave or non-s-wave superconductors.^{28–31}

A comparison of the region of superconducting fluctuations with that of cup-rate superconductors, which are known to have a short coherence length of about 10 Å,³² shows that the ZrTe₃ region is wider than that of cup-rate superconductors and comparable to that observed in the λ transition in liquid ⁴He II.³³ This result suggests that the coherence length of ZrTe₃ is extremely short and below 10 Å. On the other hand, the coherence length at 0 K, which was estimated by the anisotropic clean Ginzburg-Landau theory from the upper critical field defined as the magnetic field where the Meissner diamagnetism vanishes, is over 600 Å and much longer than the lattice constants⁵. From the contradictory estimations of the coherence length, we suggest that the very short coherence length is a feature of filamentary superconductivity rather than the fluctuations observed for the superconducting state formed below T_C . As a limit for a very short coherence length, it is reasonable to assume local pairs that interact strongly with each other in an attractive way over short distances, and that have Bose characteristics.^{34,35} Assuming that filamentary superconductivity is induced by local pairs with Bose characteristics, it would not be inconsistent with the result of the direction-dependent zero-resistance transition observed as being filamentary, because local pairs with Bose characteristics result from real space pairing. Thus, we conclude that “mixed bulk-filament superconductivity” results from a change in the pair coupling starting from local pairs with Bose characteristics to Cooper pairs. The large and widely extended tail of C_{es} may be adopted as a feature in the crossover region from superconductivity induced by local pairs to that induced by Cooper pairs.

Next we discuss the origin of the change in the pair coupling from local pairing to Cooper pairing in ZrTe₃. We notice characteristic changes in the electronic band structure across the CDW transition, in which $D(E_F)$ very close to the vHs is greatly enhanced in addition to significant electronic structural changes in the quasi-1D FS.^{16,17} It is known that the presence of a vHs at E_F can induce Fermi surface instabilities and lead to the superconducting state^{36,37} or the CDW state.³⁸ The CDW-induced enhancement in $D(E_F)$ near the vHs may lead again to superconductivity or CDW stability. Particularly, in the narrow band that constructs the quasi-1D + 3D FSs together with the wide band,^{11,16,17} electrons can form local pairs that interact attractively with each other over short

distances. In other words, the formation of local pairs of electrons with Bose characteristics will be expected.^{34,35} The local pairs formed in the narrow bands are delocalized rather than localized, because of hopping via virtual excitations into wide-band states in the quasi-1D + 3D FS. Since the narrow-band electrons have a dominant $\text{Te}5p_x$ characteristic originating in the $\text{Te}(2)\text{-Te}(3)$ chain parallel to the a axis,^{10,11} the local pairs must be dominantly formed along the a axis, leading to the zero-resistance transition of the a component. If the number of local pairs with a lower temperature increased, they would spread into a wide band in the quasi-1D + 3D FSs and induce Cooper pairs with a very short coherence length. The zero-resistance transition of the b component and the extended tail of C_{es} may be due to Cooper pairs with a very short coherence length. Furthermore, local pairs also spread into the wide band in the 3D FS and induce Cooper pairing among the wide-band electrons and vice versa.^{34,35} This mutual induction rapidly develops the coherent state of the Cooper pairs, and as a result the single-particle spectrum of the wide-band electrons opens a superconducting gap on the 3D FS, leading to the onset of the long-range order of Cooper pairs. Thus, there a crossover region appears between the superconducting state induced by local pairs and that induced by Cooper pairs in the superconducting transition of ZrTe_3 . We can conclude that “mixed bulk-filament superconductivity” results from the unique electronic structural changes in the quasi-1D + 3D FSs after the CDW transition, in which there is a large enhancement in $D(E_F)$ near the vHs and the simultaneous presence of narrow and wide bands at E_F .

The crossover from local pairs to Cooper pairs in ZrTe_3 reminds us of the Bose-Einstein condensation (BEC)-BCS crossover phenomena in ultracold atomic Fermi gases³⁹ and the BEC-BCS picture proposed in cup-rate superconductors.⁴⁰ The former is performed while varying the fermionic density or interaction and the latter while varying the hole doping. On the other hand, the crossover in ZrTe_3 is observed when the temperature is varied in the superconducting transition region. They are quite different situations, supporting the view that the unique electronic structural changes in the quasi-1D + 3D FSs after the CDW transition are deeply involved in the origin of the crossover of ZrTe_3 .

The unconventional superconducting behavior observed in ZrTe_3 , which is the reduced value of $\Delta C_e/(\gamma T_C)$, the $\gamma_0 \neq 0$ and the extended tail of C_{es} , has also been observed in non-s-wave superconductors such as heavy Fermion superconductors, the spin-triplet superconductor Sr_2RuO_4 and cup-rate superconductors.²⁸⁻³¹ These compounds are bulk superconductors where no filamentary behavior is observed, while ZrTe_3 is a “mixed bulk-filament superconductor.” Whether the unconventional behavior observed here can be explained

by non-s-wave superconductivity or “mixed bulk-filament superconductivity” will constitute a future issue. Furthermore, to confirm the nature of “mixed bulk-filament superconductivity,” ARPES and scanning tunneling spectroscopy (STS) studies will be needed at temperatures above and below T_C . A recent study has reported the coexistence of bulk superconductivity and CDW in Cu intercalated ZrTe_3 , $\text{Cu}_{0.06}\text{ZrTe}_3$.⁴¹ It is interesting to note that “mixed bulk-filament superconductivity” turns to bulk superconductivity with increasing Cu intercalation.

IV. CONCLUSION

We have shown that the superconducting transitions in ZrTe_3 are successive from filamentary to bulk, based on experimental results for a superconducting specific heat anomaly and the anisotropic superconducting transition curve of resistivity. The result shows that the superconductivity is in a mixed bulk and filamentary state, but is neither bulk nor filamentary; it can be called “mixed bulk-filament superconductivity.” A small jumplike superconducting specific-heat anomaly with a large and widely extended tail was observed to closely follow the anisotropic zero-resistance transition. We concluded that the jumplike anomaly signifies the onset of the long-range order of Cooper pairs with the opening of a superconducting gap at T_C , while the large and widely extended tail indicates superconducting behavior induced by Cooper pairs with a very short coherence length. As a limit for a very short coherence length, we proposed local pairs with Bose characteristics. The existence of local pairs can allow us to understand the direction-dependent zero-resistance transition observed in filamentary superconductivity. The large and widely extended tail of C_{es} was understood to be a superconducting feature that appears in the crossover from superconductivity induced by local pairs to that induced by Cooper pairs. The “mixed bulk-filament superconductivity” of ZrTe_3 is explained by the change in the pair coupling starting from local pairs with Bose characteristics to Cooper pairs. Based on a discussion of the origin of the change in the pair coupling from local pairing to Cooper pairing in ZrTe_3 , we concluded that the “mixed bulk-filament superconductivity” results from the unique electronic structural changes in the quasi-1D + 3D FSs after the CDW transition, where there is a large enhancement in $D(E_F)$ near the vHs and the simultaneous presence of narrow and wide bands at E_F .

ACKNOWLEDGMENTS

We are grateful to K. Inagaki and K. Ichimura for fruitful discussions. This work was supported by Hokkaido University, the 21st Century COE Program “Topological Science and Technology.”

¹J. A. Wilson and A. D. Yoffe, *Adv. Phys.* **28**, 193 (1969).

²N. P. Ong and P. Monceau, *Phys. Rev. B* **16**, 3443 (1977).

³T. Sambongi, K. Tsutsumi, Y. Shiozaki, K. Yamaya, and Y. Abe, *Solid State Commun.* **22**, 729 (1977).

⁴K. Tsutsumi, T. Takagaki, M. Yamamoto, Y. Shiozaki, M. Ido, T. Sambongi, K. Yamaya, and Y. Abe, *Phys. Rev. Lett.* **39**, 1675 (1977).

⁵S. Takahashi, T. Sambongi, and S. Okada, *J. Phys. (Paris) Colloq.* **C3**, 1733 (1983); S. Takahashi, T. Sambongi, J. W. Brill, and W. Roark, *Solid State Commun.* **49**, 1031 (1984).

⁶M. H. van Marren and G. M. Schaeffer, *Phys. Lett.* **20**, 131 (1966); *Phys. Lett. A* **24**, 645 (1967).

⁷C. Berthier, D. Jerome, P. Moline, and J. Rouxel, *Solid State Commun.* **19**, 131 (1976).

- ⁸R. Yomo, K. Yamaya, M. Abliz, M. Hedou, and Y. Uwatoko, *Phys. Rev. B* **71**, 132508 (2005).
- ⁹K. Kawabata, *J. Phys. Soc. Jpn.* **54**, 762 (1985).
- ¹⁰K. Stove and F. R. Wagner, *J. Solid State Chem.* **138**, 160 (1998).
- ¹¹C. Felser, E. W. Finckh, H. Kleinke, F. Rucker, and W. Tremel, *J. Mater. Chem.* **8**, 1787 (1998).
- ¹²H. Nakajima, K. Nomura, and T. Sambongi, *Physica B* **143**, 240 (1986).
- ¹³N. Shima, *J. Phys. Soc. Jpn.* **51**, 11 (1982).
- ¹⁴D. F. Eaglesham, J. W. Steeds, and J. A. Wilson, *J. Phys. C* **17**, L697 (1984).
- ¹⁵Y. Nogami, private communications and oral presentation at JPS meeting, 2003.
- ¹⁶T. Yokoya, T. Kiss, A. Chainani, S. Shin, and K. Yamaya, *Phys. Rev. B* **71**, 140504(R) (2005).
- ¹⁷M. Hoesch, X. Cui, K. Shimada, C. Battaglia, Shin-ichi Fujimori, and H. Berger, *Phys. Rev. B* **80**, 075423 (2009).
- ¹⁸K. Kawabata and M. Ido, *Solid State Commun.* **44**, 1539 (1982).
- ¹⁹A. J. Bevolo and H. R. Shanks, *J. Appl. Phys.* **45**, 4644 (1974).
- ²⁰W. Biberacker and H. Schwenk, *J. Solid-State Commun.* **33**, 385 (1980).
- ²¹E. Morosan, H. W. Zandbergen, B. S. Dennis, J. W. G. Bos, Y. Onose, T. Klimczuk, A. P. Ramirez, N. P. Ong, and R. J. Cava, *Nat. Phys.* **2**, 544 (2006).
- ²²N. E. Phillips, *Phys. Rev.* **114**, 676 (1959).
- ²³D. Sanchez, A. Junod, J. Muller, H. Berger, and F. Lévy, *Physica B* **204**, 167 (1995).
- ²⁴M. Morita and K. Yamaya, *Jpn. J. Appl. Phys.* **26**, 975 (1987).
- ²⁵S. Nagata, S. Ebisu, T. Aochi, Y. Kinoshita, S. Chikazawa, and K. Yamaya, *J. Phys. Chem. Solids* **52**, 761 (1991).
- ²⁶G. Kumagai, T. Matsuura, K. Ichimura, K. Yamaya, K. Inagaki, and S. Tanda, *Phys. Rev. B* **81**, 184506 (2010).
- ²⁷M. Chung, Y. Wang, J. B. Brill, T. Burgin, and L. K. Montgomery, *Synthetic Metals* **55–57**, 2755 (1993).
- ²⁸E. Bauer, G. Hilscher, H. Michor, Ch. Paul, E. W. Scheidt, A. Gribanov, Yu. Seropegin, H. Noel, M. Sigrist, and P. Rogl, *Phys. Rev. Lett.* **92**, 027003 (2004).
- ²⁹R. Movshovich, M. Jaime, J. D. Thompson, C. Petrovic, Z. Fisk, P. G. Pagliuso, and J. L. Sarrao, *Phys. Rev. Lett.* **86**, 5152 (2001).
- ³⁰A. P. Mackenzie and Y. Maeno, *Rev. Mod. Phys.* **75**, 657 (2003).
- ³¹J. W. Loran, K. A. Mirza, K. A. Wade, J. R. Cooper, and W. Y. Liang, *Physica C* **235**, 134 (1994).
- ³²M. Casas, J. M. Getino, M. de Llano, A. Puente, R. M. Quick, H. Rubio, and D. M. van der Walt, *Phys. Rev. B* **50**, 15945 (1994).
- ³³G. Ahlers, *Phys. Rev. A* **3**, 696 (1971).
- ³⁴S. Robaszkiewicz, R. Micnas, and J. Ranninger, *Phys. Rev. B* **36**, 180 (1987).
- ³⁵J. Ranninger, J. M. Robin, and M. Eschrig, *Phys. Rev. Lett.* **74**, 4027 (1995).
- ³⁶J. Labble and J. Friedel, *J. Phys. (Paris)* **27**, 153 (1966).
- ³⁷J. Labble and J. Bok, *Europhys. Lett.* **3**, 1225 (1987).
- ³⁸T. M. Rice and G. K. Scott, *Phys. Rev. Lett.* **35**, 120 (1975).
- ³⁹M. Greiner, C. A. Regal, and D. S. Jin, *Nature (London)* **426**, 537 (2003); C. Chin, M. Bartenstein, A. Altmeyer, S. Riedl, S. Jochim, J. H. Denschlag, and R. Grimm, *Science* **305**, 1128 (2004); M. W. Zwierlein, J. R. Abo-Shaeer, A. Schirotzek, C. H. Schunck, and W. Ketterle, *Nature (London)* **435**, 1047 (2005).
- ⁴⁰Y. J. Uemura, *Physica C* **282**, 194 (1997).
- ⁴¹X. Zhu, H. Lei, and C. Petrovic, *Phys. Rev. Lett.* **106**, 246404 (2011).